New Improvements in the C6 MODIS Land-Surface Temperature Product

Zhengming Wan

ERI, University of California, Santa Barbara, CA 93106, USA

Basic Considerations in MODIS LST Algorithms

1. LST is retrieved from TIR data only in clear-sky conditions.

LST is not mixed with cloud-top temperature in the atmospheric product.

2. LST is defined by the radiation emitted by the land surface observed by MODIS at the instantaneous viewing angle.

Applications may need LST at different angles (nadir or 50^{o} from nadir).

3. Proper resolving of the land-atmosphere coupling is the key in retrieving surface & atmospheric properties. Use multi-bands in the atmospheric windows for the LST retrieval.

The atmospheric temperature and water vapor are useful to improve the LST retrieval. But there may be large errors in these values. Use them as indicates of ranges or initial guesses.

4. The split-window LST algorithm is the primary algorithm to generate MODIS LST products including the level-2 product (M*D11_L2) and the 1km level-3 product (M*D11A1) because surface emissivities vary within narrow ranges in the spectral ranges of MODIS bands 31 and 32 for all land-cover types. The day/night algorithm is used to retrieve surface emissivity values.

5. Surface emissivities do not significantly change with time because thermal infrared radiation almost does not penetrate a thin vegetation leaf (about 0.18mm thick) and its reflectance does not change with the water content in the leaf in the spectral range above 7μm.

6. Input data: M*D021KM, M*D03, M*D07, M*D10, M*D12, M*D35 & M*D43.

Reflectance spectra measured from sand and soil samples by the MODIS LST group. There are significant variations in the ranges of 3-5 and 8-10μm (left). The changes in the reflectance/emissivity difference in bands 31 and 32 (at 11 and 12μm shown in right) are in a relatively narrow range.

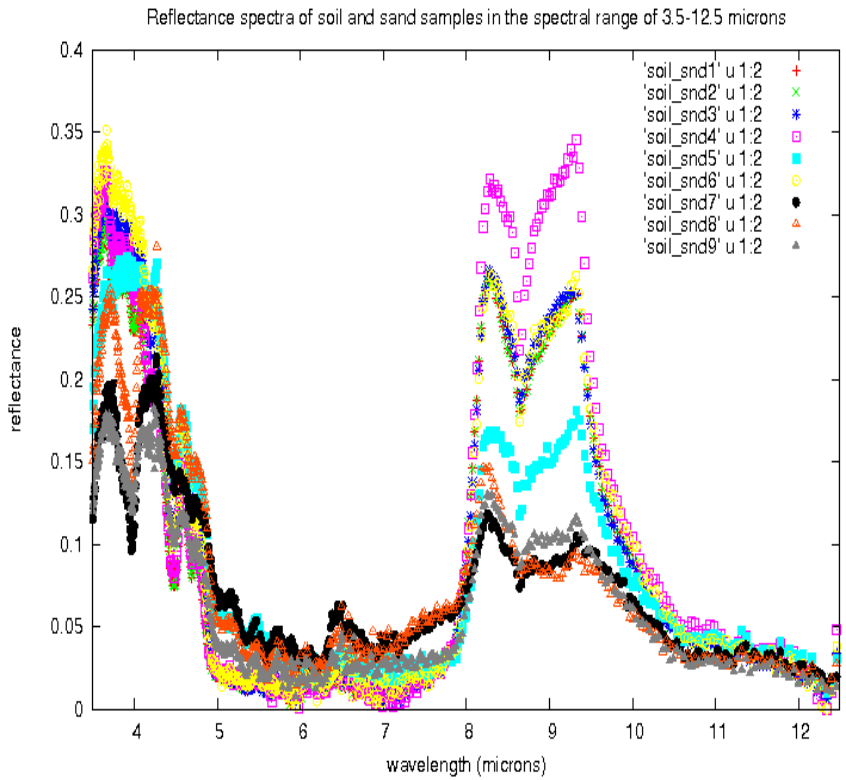

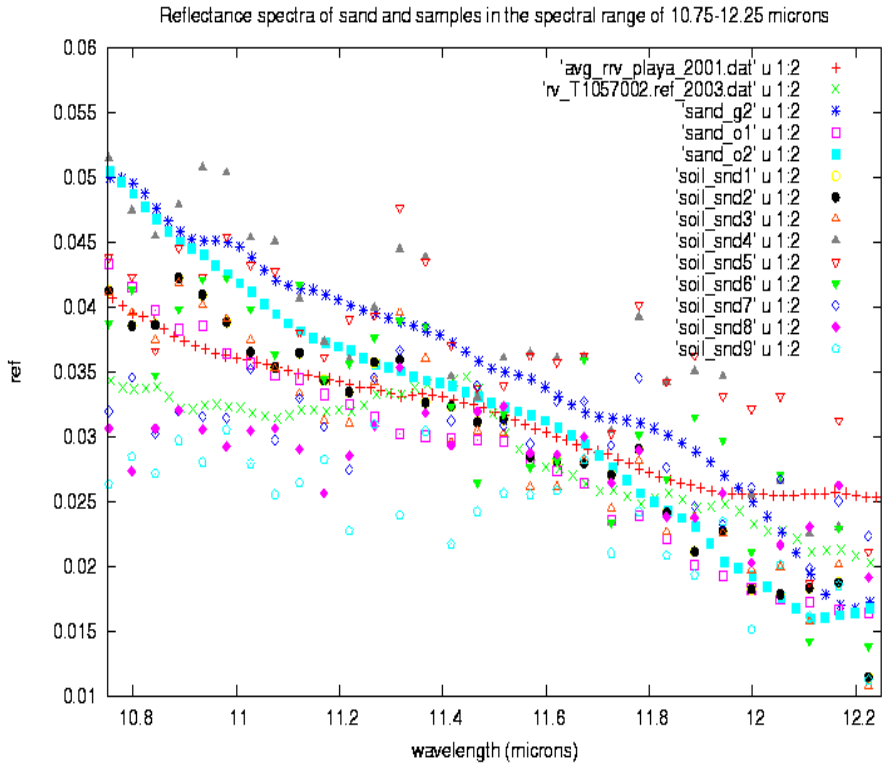

According to the left plot, the emissivity values of soil and sand samples in MODIS bands 20/22 and 29 vary in range of 0.65 – 0.92. This range may be used as a useful reference in evaluation of retrieved emissivity values in arid regions.

The 0.015 variation range of emissivity values in MODIS bands 31 and 32 for soil and sand samples means relatively larger errors in LSTs retrieved by the split-window algorithm in arid regions compared to water and vegetated surfaces.

MODIS LST Algorithms (I)

The generalized split-window algorithm (Wan and Dozier, 1996) is in form

$$T_s = C + \left(A_1 + A_2 \frac{1-\varepsilon}{\varepsilon} + A_3 \frac{\Delta\varepsilon}{\varepsilon^2} \right) \frac{T_{11\mu} + T_{12\mu}}{2} + \left(B_1 + B_2 \frac{1-\varepsilon}{\varepsilon} + B_3 \frac{\Delta\varepsilon}{\varepsilon^2} \right) \frac{T_{11\mu} - T_{12\mu}}{2}$$

where $\varepsilon = 0.5\,(\varepsilon_{11\mu} + \varepsilon_{12\mu})$ and $\Delta\varepsilon = \varepsilon_{11\mu} - \varepsilon_{12\mu}$

$T_{11\mu} - T_{12\mu}$ also expressed as $T_{31} - T_{32}$ for MODIS.

- emissivities estimated from land cover types (**Snyder et al., 1998; Snyder & Wan, 1998**).

  Emissivities vary slightly even within a land cover type (crop lands may have different soils and crops in variable coverage).

  A MODIS pixel may cover several 1km grids with different land cover types.

- coefficients Ai, Bi, and C depend on viewing zenith angle (in range of 0-65^o).
- coefficients also depend on ranges of the air surface temperature and column water vapor.
- only process pixels in clear-sky at different M*D35 confidences over land or in lakes.

MODIS LST Algorithms (II)

The MODIS day/night LST algorithm (Wan & Li, 1997) is performed for grids larger than MODIS pixels:

- retrieve Ts-day, Ts-night, & band emissivities simultaneously with day & night data in seven bands (bands 20, 22, 23, 29, and 31-33).
- be able to adjust the input atmospheric cwv and Ta values.
- least square-sum fitting 14 observations to solve 13 variables: Ts-day, Ts-night, cwv and Ta values for day and night, emissivities in the first six bands (small surface effect in b33) and a BRDF factor in the first three bands.
- The range of viewing zenith angle is separated into 16 sub-ranges in v5 (5 sub-ranges in v4).
- Option for combined use of Terra and Aqua MODIS data in v5.
- Terrain slope is considered in v5 QA.

Highlights of the C6 Daily MODIS LST PGE (PGE16)

1, Executive 1, input M*D02, M*D03, M*D07, M*D10 and M*D35 granule by granule, apply the split-window algorithm to generate M*D11_L2 and L3 M*D11A1 and M*D11B1 products, and store the data in seven TIR bands, BRDF factor of band 7 in the BRDF product, solar and viewing angles and atmospheric cwv and Ta_surf data to the continuously updated UPD tile files. The landcov and BRDF tile files kept at the same fixed order in the pcf are read in only necessarily. The information of snow and lake ice only given in the daytime granules is also kept in the UPD files and will be used in the processing of consequent nighttime granules.

2, Executive 2, apply the day/night algorithm tile by tile with the information stored in the UPD files, use the accumulated em20, em22 and em29 values in UPD files as initial values optionally, and update these values after getting a successful solution. The retrieved daytime and night time LSTs and emis values with observation time/angle are outputted to M*D11B1.

3, Executive 3, remove cloud-contaminated data in M*D11A1 files by analyzing the LST data in 32 days.

4, Executive 4, remove cloud-contaminated data in M*D11B1 files by analyzing the LST data in 32 days.

5, Because of the above reasons and the UPD's need for storing information in 32 days, the previous 32 days should be processed when a new processing stream is started. The UPD files are necessary due to its multiple functions. Its primary function is to serve as the database for pairs of day and night MODIS observations in up to 16 zenith angle sub-ranges.

Radiance-based approach to valid LSTs (Wan and Li, 2008)

1. **It uses surface emissivity spectra measured or estimated, and atmospheric temperature and water vapor profiles in atmospheric radiative transfer simulations to invert the band-31 brightness temperature of MODIS observation to a LST value, and compare this value with the LST value in the MOD11 product.**
2. **This approach works because of high calibration accuracies in bands 31 & 32.**
3. **This approach has been validated by comparisons to the conventional temperature-based approach in large homogeneous fields (lakes, grassland, and rice fields) by the MODIS LST group and the César Coll's group.**
4. **It is better than the conventional temperature-based approach because the large spatial variation in LSTs especially in the daytime makes it impossible to measure LSTs at 1km scale and the small horizontal variations in atmospheric temperature and water vapor profiles in clear-sky conditions support the R-based approach.**
5. **It is important to use the atmospheric profiles appropriate to the MODIS observations by constraints of time (within 2-3 hours) and distance (≤ 100km).**
6. **It is important to perform the R-based approach on a series of days and to make quality control by comparing the values of (Tb31 – Tb32) in the simulations and MODIS observations and utilizing the difference d(Tb31 – Tb32) values in QC.**
7. **The R-based approach may not work well in wet conditions or partly cloudy days because the atmospheric profiles measured by balloons may be very different from the real profiles along the paths of MODIS observations, and clouds and heavy aerosols are not included in radiative transfer simulations. For example, as surface visibility changes from 23km to 1km, Tb31 decreases by 1.5K.**

A list of the validation sites used in the past for the C5 (V5) MODIS LST products

Site	Location	Latitude, Longitude (°)	Landcover Type	Type of Validation	References
1	Lake Titicaca, Bolivia	16.247 S, 68.723 W	in-land water (0)	T-based and R-based	Wan et al (2002); Wan (2008)
2	Mono Lake, CA	38.01 N, 118.97 W	in-land water (0)	T-based	Wan et al (2002); Wan (2008)
3	Walker, NV	38.697 N, 118.708 W	in-land water (0)	T-based	Wan et al (2002); Wan (2008)
4	Salton Sea, CA	33.2 N, 115.75 W	in-land water (0)	R-based	Wan & Li (2008)
5	near Salton Sea, CA	33.25 N, 115.95 W	bare soil (16)	R-based	Wan & Li (2008)
6	Bridgeport, CA	38.22 N, 119.268 W	grassland (10)	T-based and R-based	Wan et al (2002); Wan (2008)
7	grassland, TX	36.299 N, 102.571 W	grassland (10)	R-based	Wan & Li (2008)
8	Railroad Valley, NV	34.462 N, 115.693 W	silt playa (16)	T-based and R-based	Wan et al (2002); Wan & Li (2008)
9	soybean field, Mississippi	33.083 N, 90.787 W	cropland (12)	T-based	Wan et al (2004); Wan (2008)
10	rice field, Valencia, Spain	39.265 N, 0.308 W	cropland (12)	T-based and R-based	Coll et al (2005); Wan & Li (2008)

Validation of the C5 LST Products generated in V5 tests

(at the ten validation sites)

By comparisons of LST values in the C5 MOD11_L2 and MYD11_L2 products with the in-situ values in Wan et al., 2002; Wan et al., 2004; Coll et al., 2005, and radiance-based validation results over Railroad Valley, NV in June 2003 and a grassland in northern TX in April 2005. LST errors < 1K in most cases.

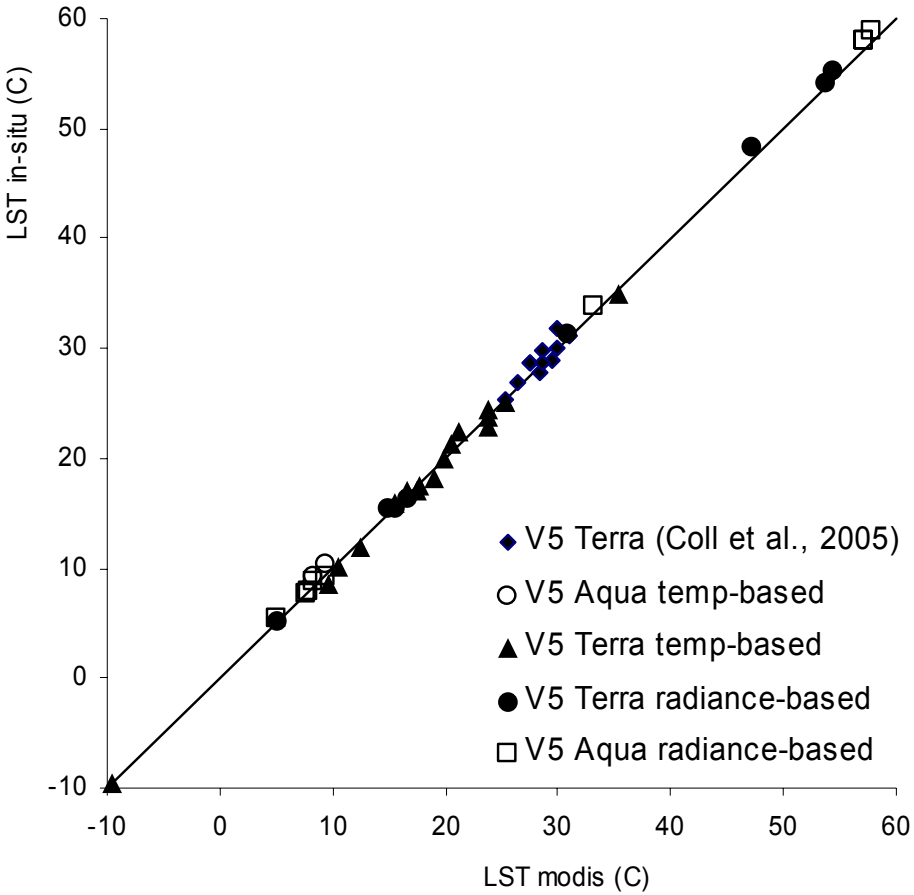

Notes for applications of C4 & C5 LST products:

- In M*D11_L2, if valid LSTs are available in both C4 & C5, their difference is less than 0.2-0.4K in most cases.

- In M*D11A1 within latitude ±28º(MODIS orbits w/o overlapping), if valid LSTs are available in both C4 & C5, their difference is less than 0.2-0.4K in most cases. Outside the latitude region, if valid LSTs are available in both C4 & C5 and at the same view time (indicating temporal average not applied in C4), their difference is less than 0.2-0.4K in most cases. Users should remove cloud-contaminated LSTs in the C4 product before using them in applications.

- LSTs severely contaminated by clouds were removed from level-3 C5 products, but not from all C4 products.
It is very difficult to remove such LSTs from the 8-day C4 M*D11A2 products because the cloud contamination effect may be reduced in the 8-day averaging.

See details in Wan (2008) and Wan and Li (2008)

The summary of R-based validation of the C5 (V5) MODIS LST products at new sites

Site	Location	Latitude, Longitude (°)	Land-cover Type (id #)	MOD11 or MYD11_L2	type of atmos. profiles	mean (std) of LST errors (K)
11	Recife, Brazil	7.96 S, 34.94 W	evergreen forest (2)	MOD11	radiosonde	0.4 (0.4)
12	Moree, Australia	29.555 S, 149.86 E	open shrubland (7)	MOD11	radiosonde	-0.8 (0.9)
13	Port Elizabath, S. Africa	33.95 S, 23.59 E	evergreen forest (2)	MYD11	radiosonde	-0.2 (0.9)
14	WLT Alert,Canada	82.4 N, 62.33 W	shrubland (7)/snow(15)	MOD11	radiosonde	0.2 (0.8)
15	South Pole	89.95 S, 0.05 E	snow/ice (15)	MOD11	radiosonde	-0.5 (0.6)
16	McMurdo,Antarctica	77.75 S, 164.1 E	snow/ice (15)	MOD11	radiosonde	0.1 (0.3)
17	Dye-2, Greenland	66.481 N, 46.28 W	snow/ice (15)	MOD11	NCEP	0.0 (0.5)
18	Summit, Greenland	72.58 N, 38.475 W	snow/ice (15)	MOD11	NCEP	0.1 (0.5)
19	Cherskij, Russia	68.75 N, 161.27 E	snow (15)/shrubland(7)	MOD11	radiosonde	0.3 (0.5)
20	Gaze, Tibet, China	32.3 N, 84.06 E	open shrubland (7)	MOD11	NCEP	-0.6 (0.2)
21	Hainich, Germany	51.079 N, 10.452 E	mixed forest (5)	MOD/MYD	radiosonde	-0.3 (0.5)
22	Paris, France	48.8 N, 2.35 E	urban (13)	MYD11	radiosonde	0.1 (0.4)
23	near Paris, France	48.45 N, 2.25 E	cropland (12)	MYD11	radiosonde	0.0 (0.6)
24	Nimes, France	43.84 N, 4.37 E	urban (13)	MYD11	radiosonde	0.1 (0.4)
25	near Nimes, France	43.828 N, 4.535 E	cropland (12)	MYD11	radiosonde	-0.1 (0.6)
26	Milan, Italy	45.485 N, 9.21 E	urban (13)	MYD11	radiosonde	-0.3 (0.7)
27	near Milan, Italy	45.297 N, 9.26 E	cropland (12)	MYD11	radiosonde	-0.3 (0.6)
28	Cuneo, Italy	44.53 N, 7.62 E	cropland (12)	MYD11	radiosonde	0.0 (0.5)
29	Payerne, Switzerland	46.855 N, 6.965 E	cropland (12)	MYD11	radiosonde	0.0 (0.5)
30	Nenjiang, China	49.07 N, 125.23 E	cropland(12)/snow(15)	MOD11	radiosonde	-0.3 (0.6)
31	Yichun, China	47.76 N, 128.88 E	mixed forest (5)	MOD11	radiosonde	0.1 (0.6)
32	Harbin, China	45.73 N, 126.65 E	urban (13)	MOD11	radiosonde	0.2 (0.8)
33	near Harbin, China	45.9 N, 127.1 E	cropland (12)	MOD11	radiosonde	0.1 (0.8)
34	Algiers, Algeria	36.72 N, 3.03 E	urban (13)	MOD11	radiosonde	-0.2 (0.9)
35	Dar-El-Beida,Algeria	36.65 N, 3.28 E	cropland (12)	MOD11	radiosonde	-0.5 (0.7)
36	Niamey, Niger	13.5 N, 2.14 E	urban (13)	MOD11	radiosonde	-0.3 (1.0)
37	Near Niamey, Niger	13.58 N, 2.07 E	grassland (10)	MOD11	radiosonde	-0.9 (1.1)
38	Tamanrasset, Algeria	22.856 N, 5.455 E	bare soil (16) in desert	MOD/MYD	radiosonde	-1.9 (1.2)
39	Bechar, Algeria	31.62 N, 2.33 W	bare soil (16) in desert	MOD/MYD	radiosonde	-1.5 (0.6)
40	Farafra, Egypt	27.04 N, 27.97 E	bare soil (16) in desert	MYD11	radiosonde	0.9 (0.4)
41	SVU, Egypt	26.285 N, 32.78 E	bare soil (16) in desert	MYD11	radiosonde	-1.6 (0.5)
42	In-salah, Algeria	27.18 N, 2.6 E	bare soil (16) in desert	MOD/MYD	radiosonde	-3.0 (0.8)

New Improvements for the C6 LST Product

(1) Generate separate sets of coefficients for the viewing-angle dependent split-window algorithm over bare soil regions during daytime and nighttime. A square term of the brightness temperature difference was added to improve the accuracy slightly. The range of (LST – Ts-air) is set as from 8 – 29K for daytime LST and from -10 – 4K for nighttime LST.
This refinement significantly improved the LST retrieval, reducing the mean (std) of LST errors in the last column of the table in the previous page to -0.2 (0.5), -0.4 (0.4), -0.2 (0.4), 0.3 (0.5)K at the bare soil site west of Salton Sea and sites 38 and 39 and 41, but not so good at sites 40 and 42 where the mean (std) values are 2.8 (0.7) & -1.4 (0.6)K due to possible large errors in em31 em32.

(2) Tune the day/night algorithm to improve its performance in desert regions, keeping the good V5 performance in lakes and forest/vegetation regions.

(3) Not mix retrieved emis values from pairs of current day and previous night observations with those from pairs of current night and previous day observations in order to preserve the angular dependence in emis values, and add em22_nit & em29_nit into M*D11B1.

(4) Store averaged em20, em22 & em29 in the UPD files and use them as initial values in the day/night algorithm to improve their accuracies.

(5) Add 8-day M*D11B2 and monthly M*D11B3 product into the MODIS LST Suite.

New Improvements for the C6 LST Product (cont.)

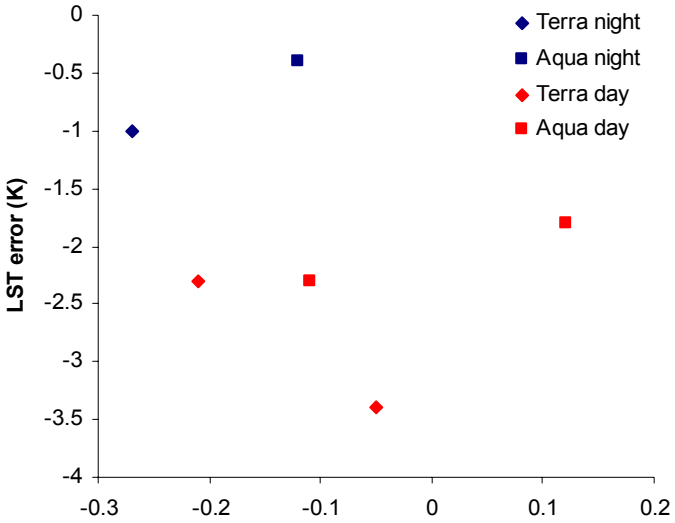

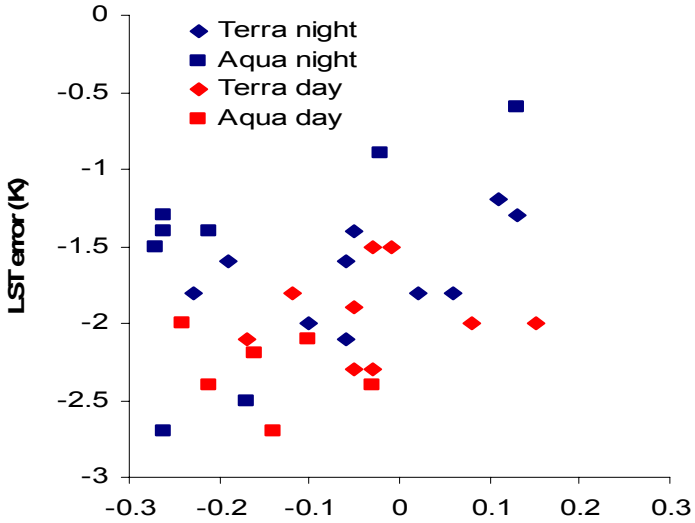

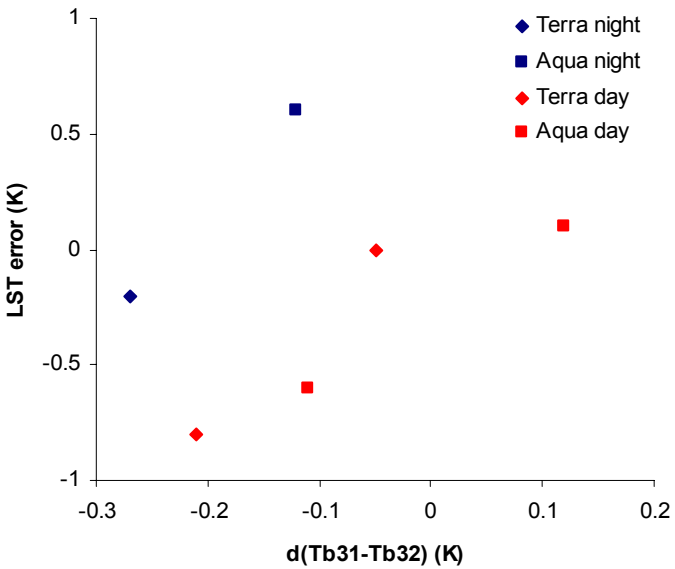

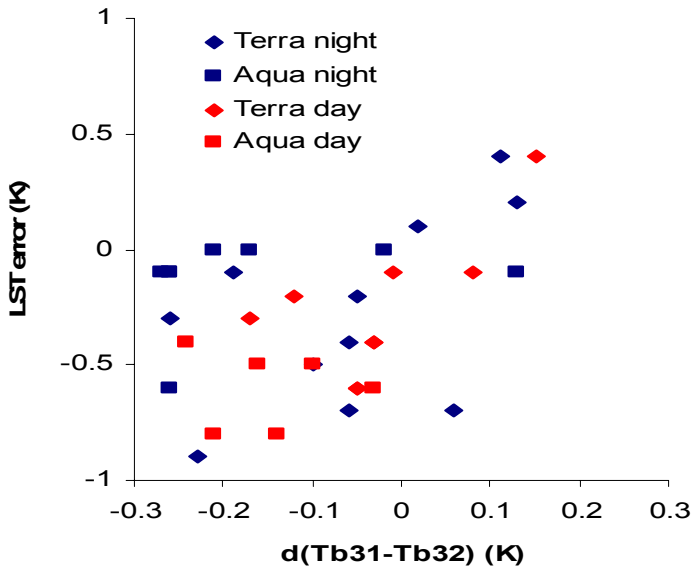

LST errors at site 5 (bare soil site west of Salton Sea) in V5 (upper) and V6 (bottom).

LST errors at site 38 (Tamanrasset) in V5 (upper) and V6 (bottom).

New Improvements for the C6 LST Product (cont.)

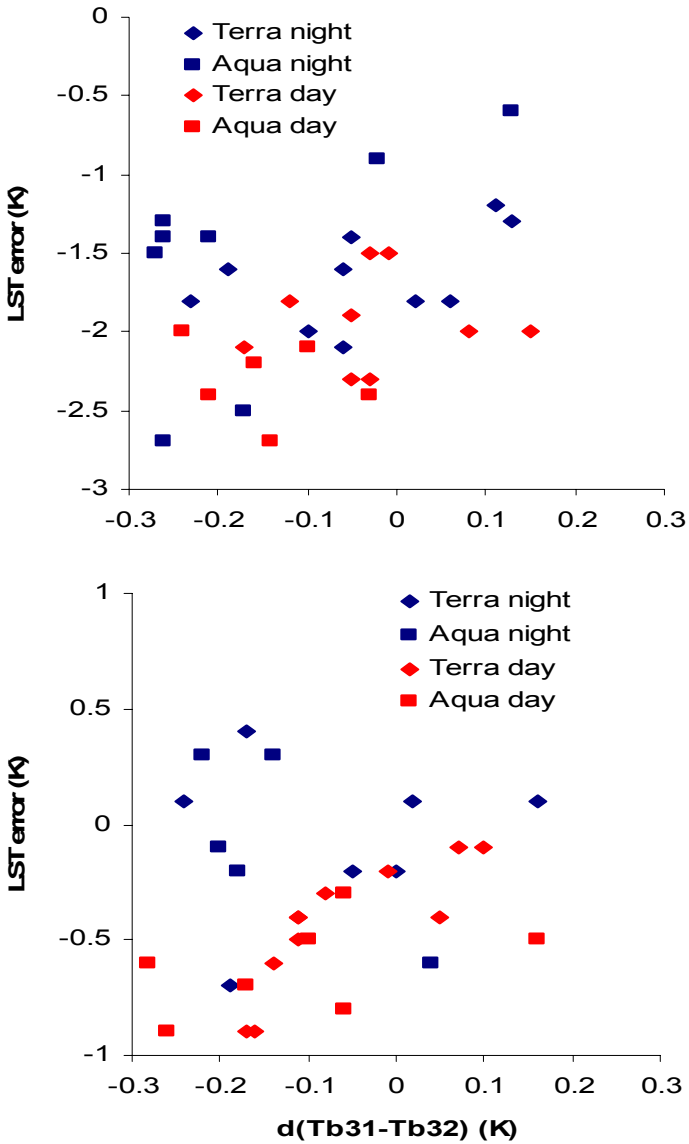

LST errors at site 39 (Bechar) in V5 (upper) and V6 (bottom).

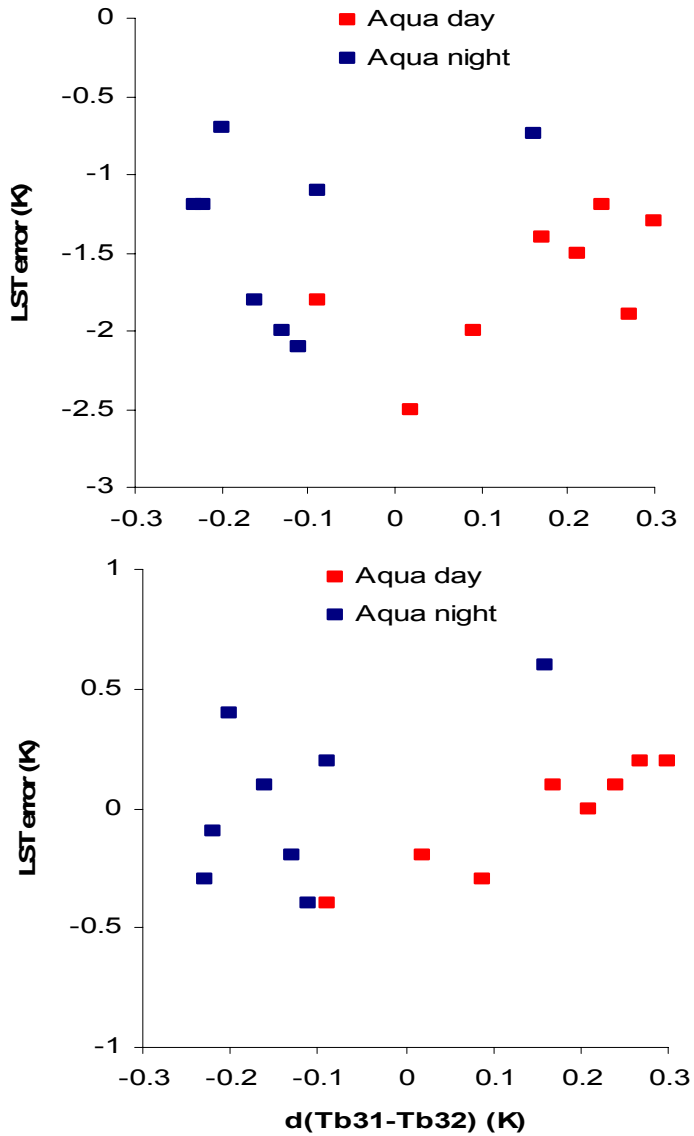

LST errors at site 41 (South of Valley Univ.) in V5 (upper) and V6 (bottom). NCEP profiles were used in the nighttime cases at this site.

Comparison between V5 and V6 daytime LSTs at three bare soil sites in North Africa

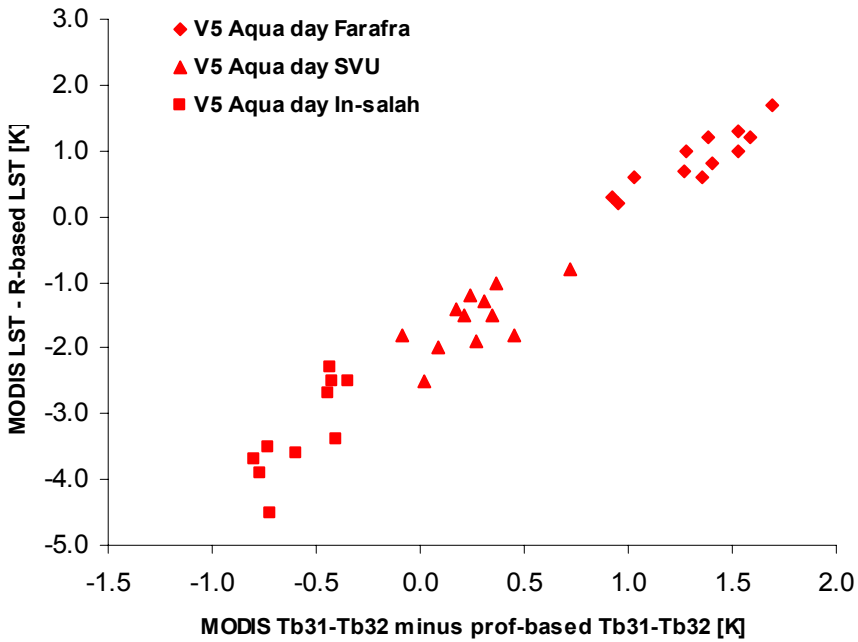

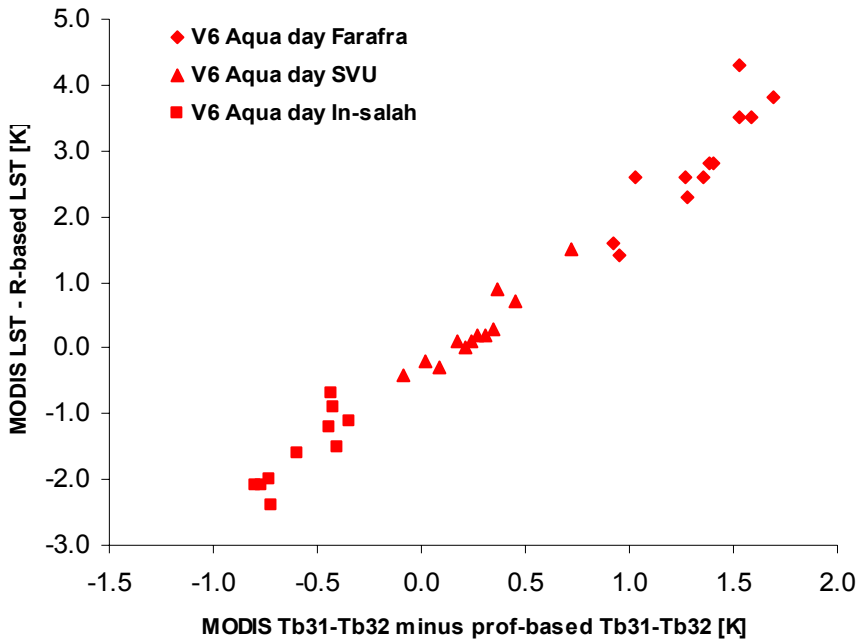

Comparison of errors in daytime Aqua MODIS LSTs at sites 40-42 (Farafra, SVU, and In-salah) in V5 (left) and V6 (right) indicates that V6 LSTs are about 2K higher than V5 LSTs and that the similar linear relation between LST errors and d(Tb31 – Tb32) values is mainly due to the differences in surface emissivities in bands 31 and 32 at the three bare soil sites.

Comparison of C6 LST Product to C5 and C41 (1)

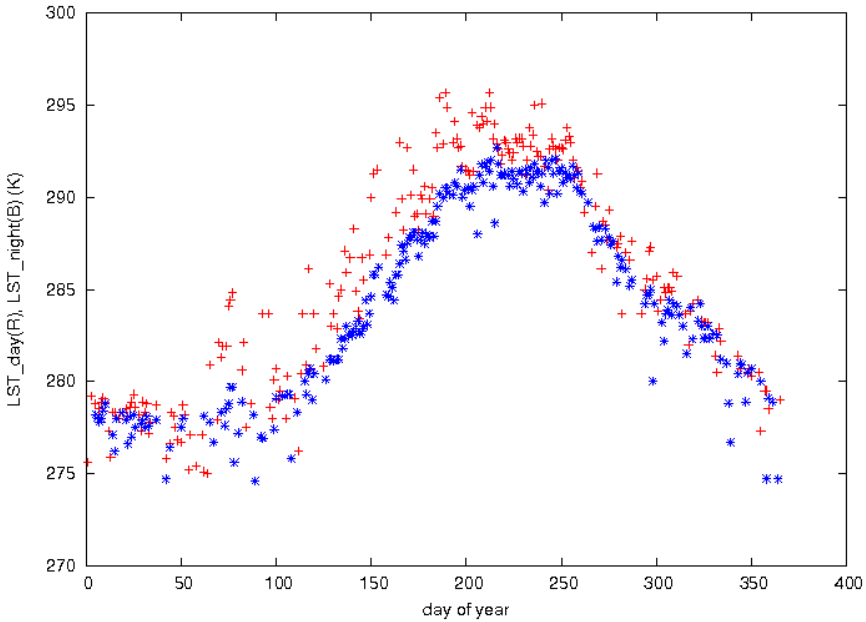

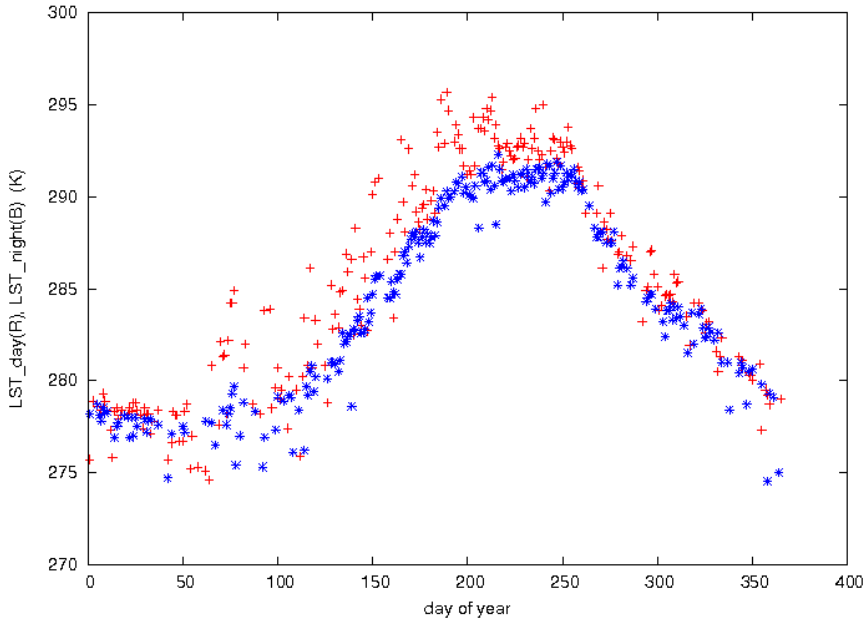

LST_day (red) and LST_night (blue) at Lake Tahoe, CA, retrieved by the day/night algorithm in the MYD11B1 product in 2007 in C6 (above), C5 (upper right) and C41 (lower right).

Note that Lake Tahoe does not freeze in the whole year so the low LST values in the C41 are due to cloud contaminations.

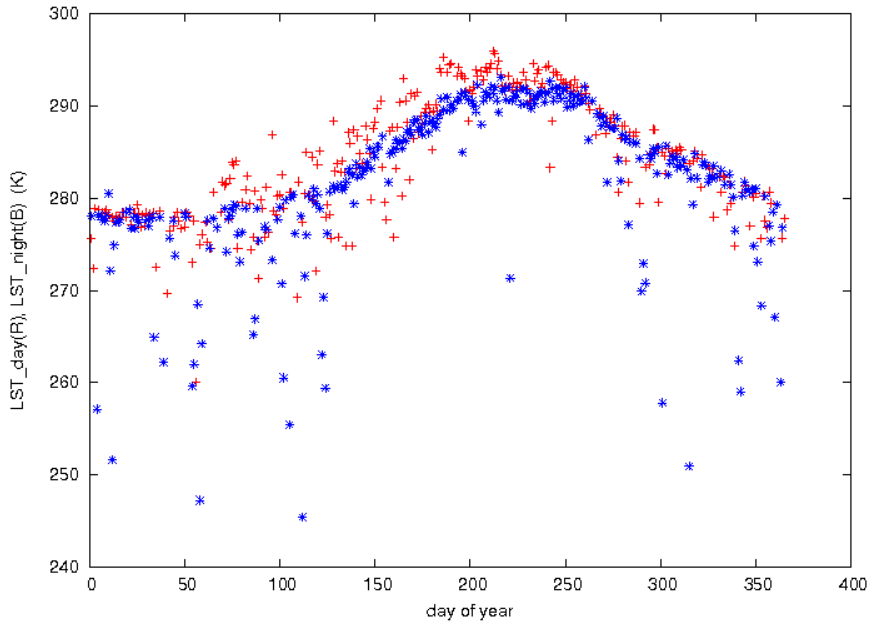

Comparison of C6 LST Product to C5 and C41 (2)

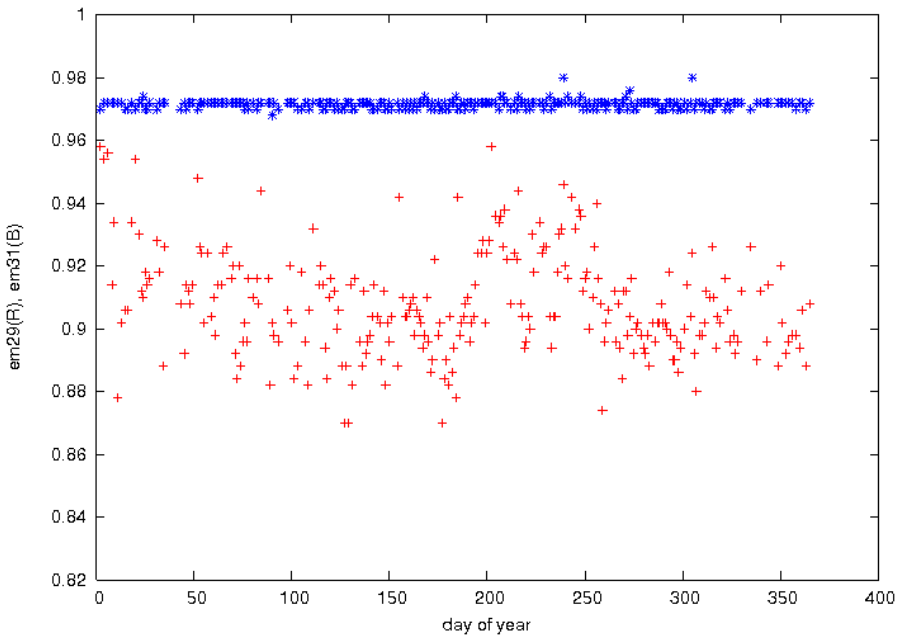

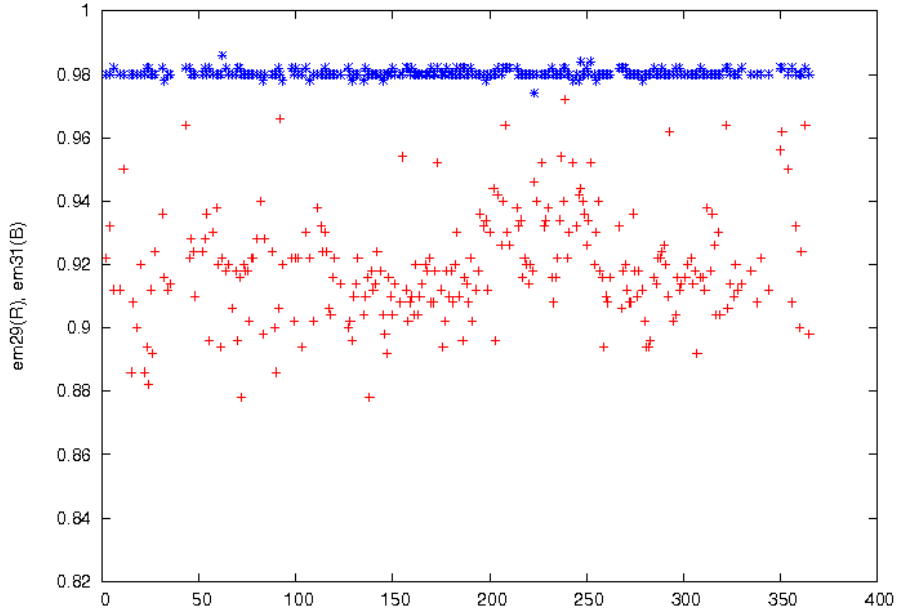

em29 (red) and em31 (blue) at a shrubland in Mojave, CA, retrieved by the day/night algorithm in the MYD11B1 product in 2007 in C6 (above), C5 (upper right) and C41 (lower right).

Many emissivity values in the C41 are too low, which would correspond to unreasonably high LSTs.

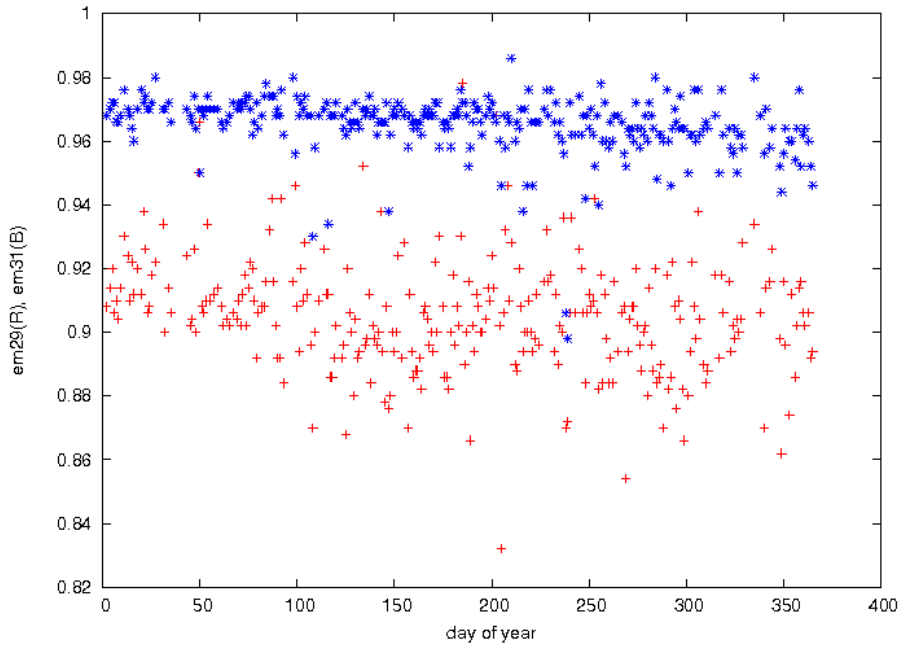

The effect of new C6 L1B data on the LST retrieval

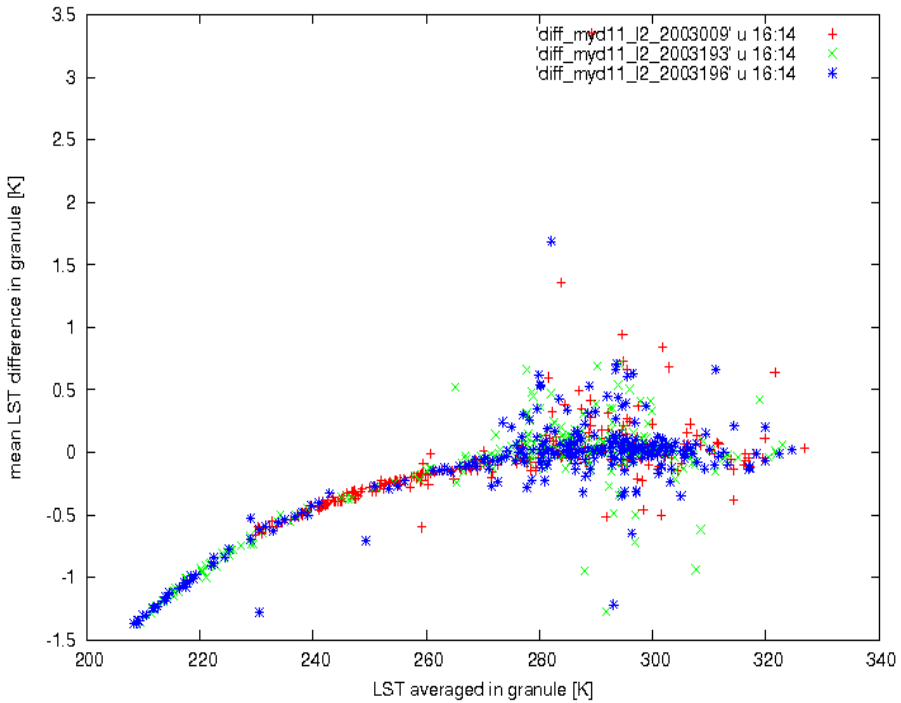

The above plot shows the mean LST difference in granule vs LST averaged in granule based on MYD11_L2 data in AS409 and AS422. The trend curve indicates that the new C6 L1B data do not change the LSTs retrieved from data of bands 31 and 32 in range of 280-330K but it reduces the LST in cold regions by 1.3K around 208K at most. The scatter points departed from the trend curve represent the effect of the different column water and surface air temperature values in the C5 and C6 MYD07_L2 products on the LST retrieval of a small number of pixels near clouds in wet conditions, especially at large viewing zenith angles by swath edges.

$T(0.3L_{typ})$ $T(L_{typ})$ $T(0.9L_{max})$

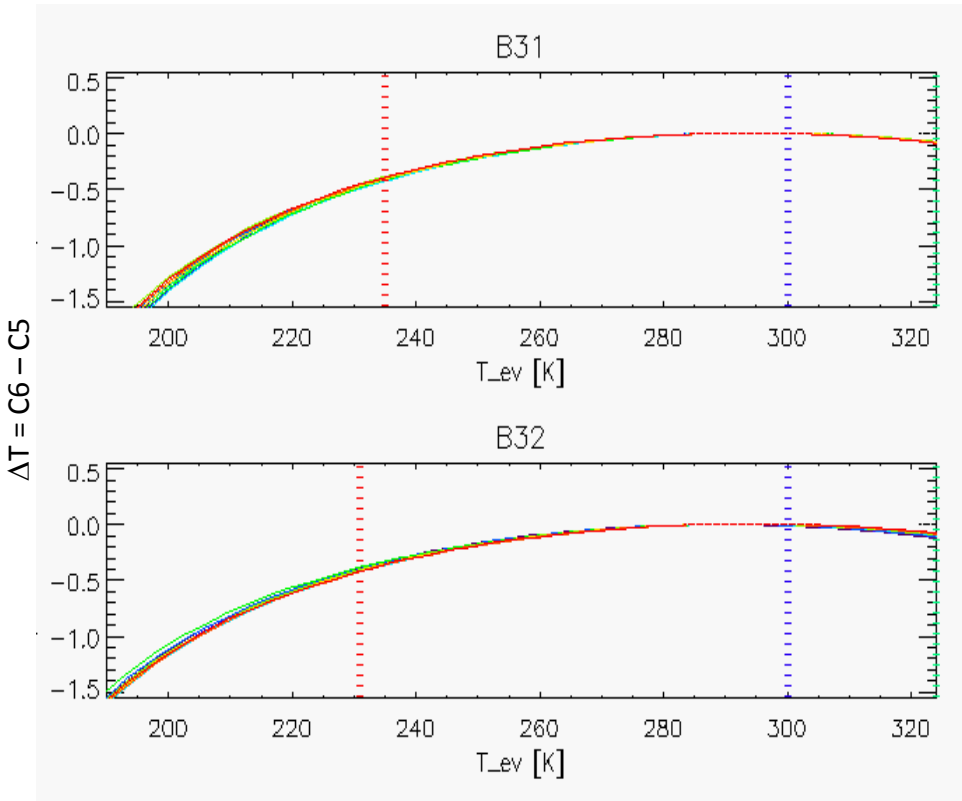

C6 Test Granule 2012088.0950

Courtesy of Brian Wenny [brian.wenny@sigmaspace.com]

Therefore, the validation results of the C5 LSTs retrieved By the split-window algorithm in range of 280-330K are also valid for corresponding C6 LSTs.

Comparison of the color composite with em22, em29 and 31 as RGB in h16-21v04-07 in the C6 MYD11B1 (top left) to C5 (top right) during 1/1-24/2003, and C41 during 1/1-24/2007 (bottom left)

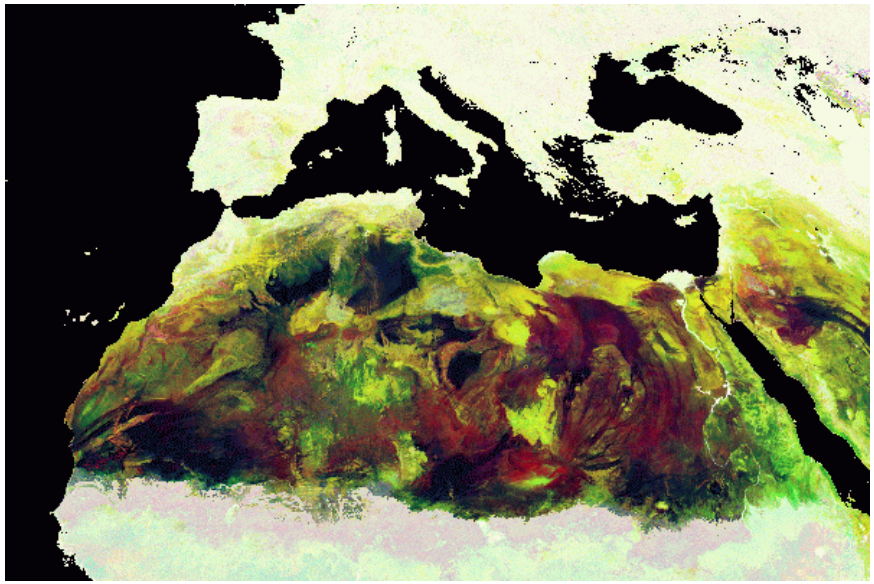

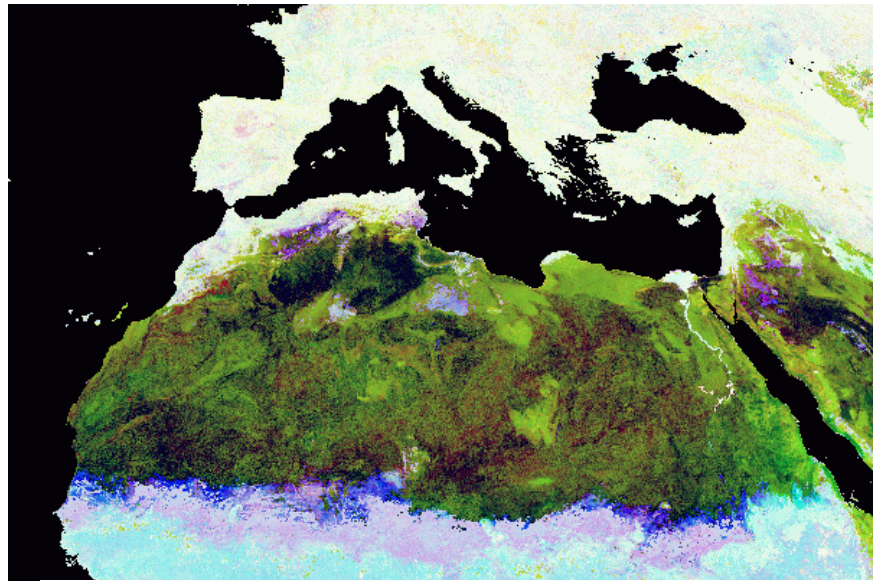

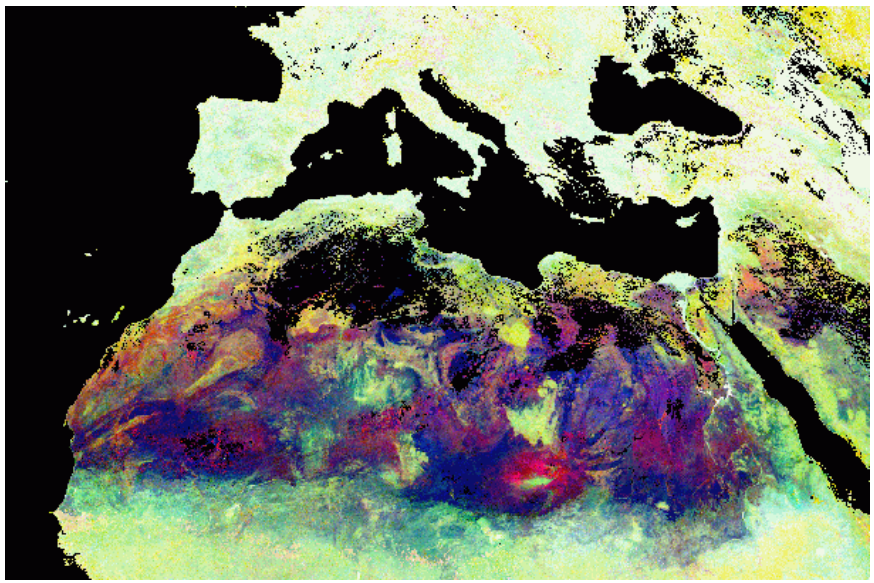

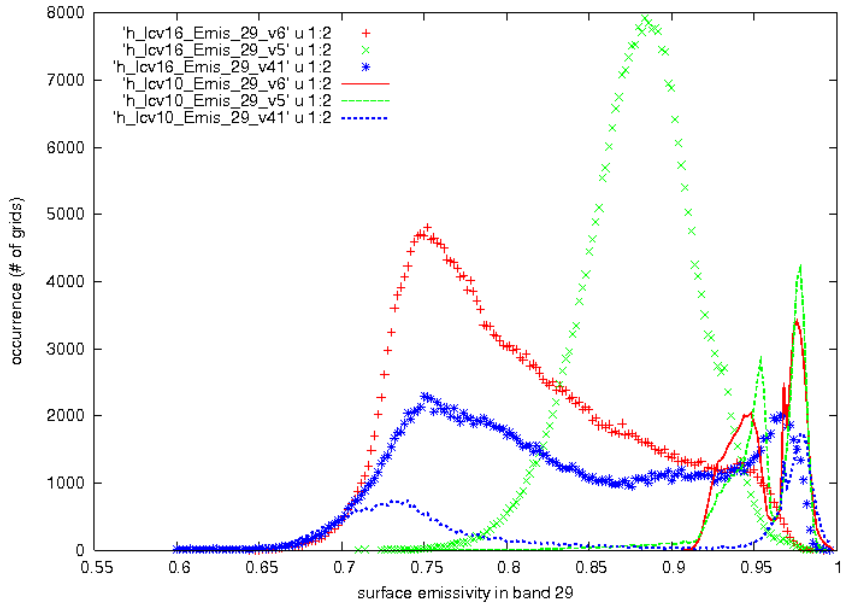

The Emis_29 values in C6 M*D11B1 are more closer to those in C41M*D11B1 in arid regions (lcv16), but more closer to those in C5 M*D11B1 in grasslands (lcv10). So C6 M*D11B1 is better than both C41 and C5.

Go to details in one tile h17v06 for comparison of the color composite with em22, em29 and 31 as RGB in the C6 MYD11B1 during 1/1-24/2007 (top left) to C5 (top middle), and C41 (top right)

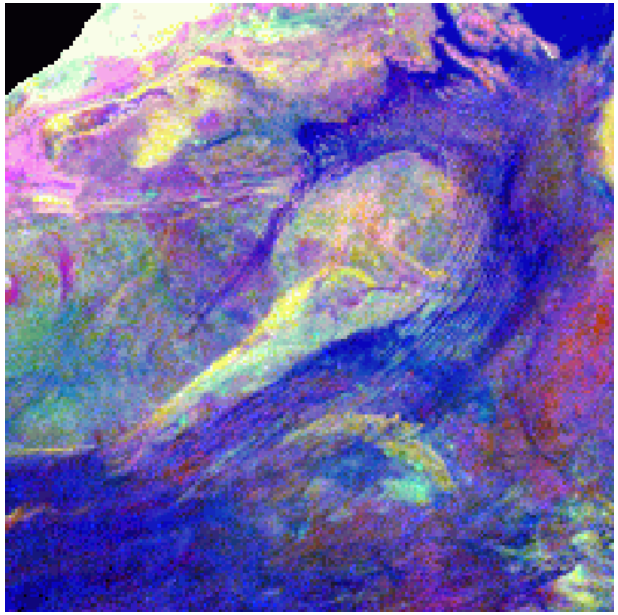

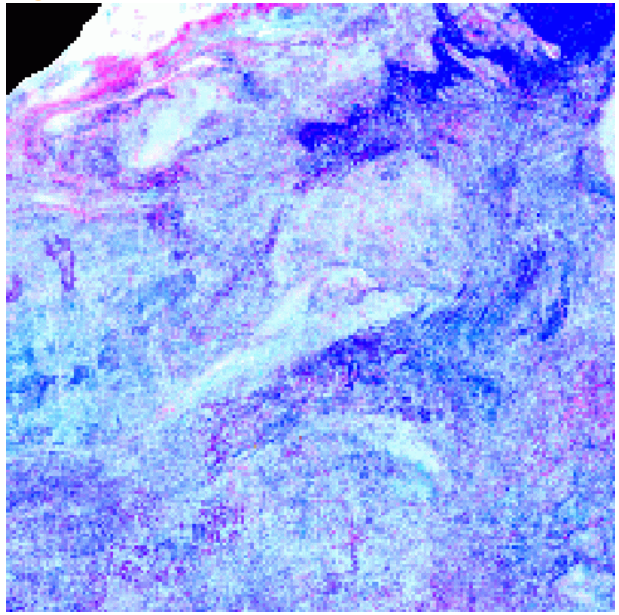

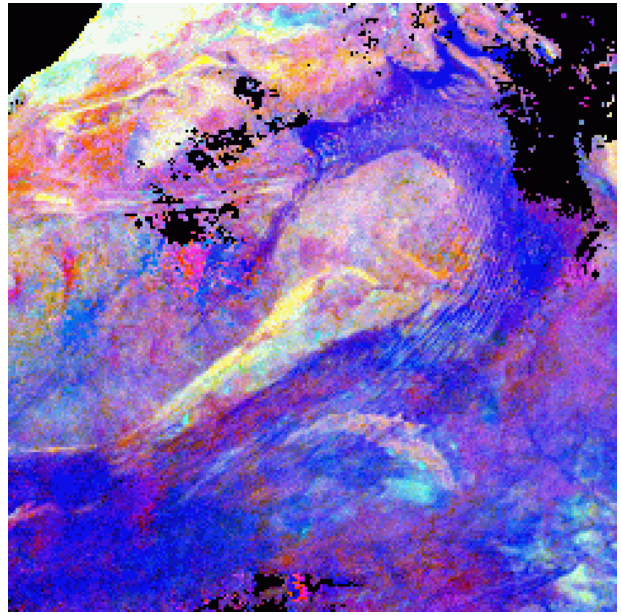

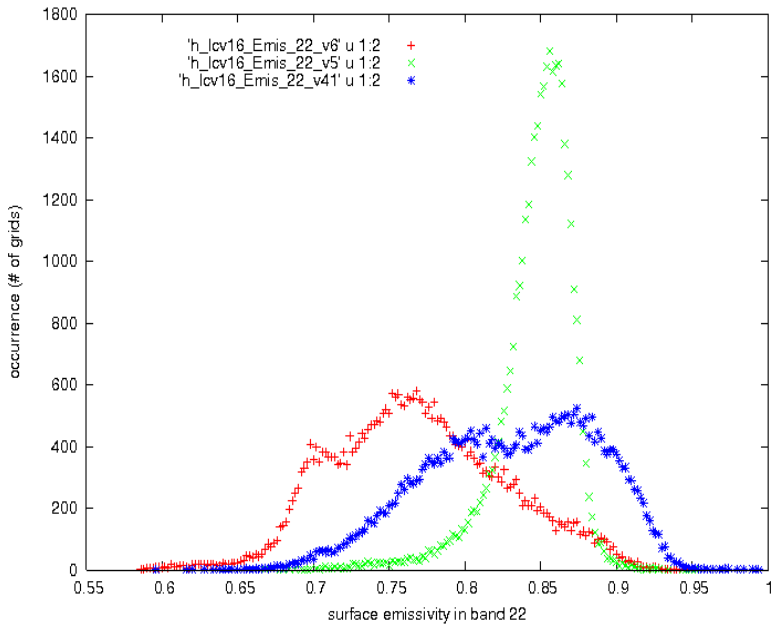

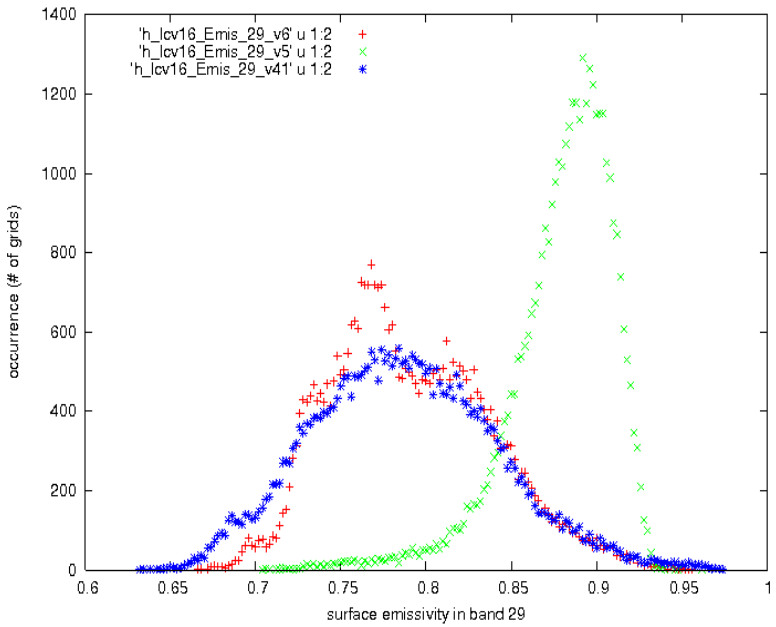

The values of Emis_22 and Emis_29 in C5 are too high here. The C6 is close to C41 & better than C41 in full spatial coverage -Indicating good performance of the V6 day/night algorithm. In-situ validation Is desirable.

Go to details in tile h08v05 for comparison of the color composite with em22, em29 and 31 as RGB in the C6 MYD11B1 during 1/1-31/2007 (top left) to C5 (top middle), and C41 (top right)

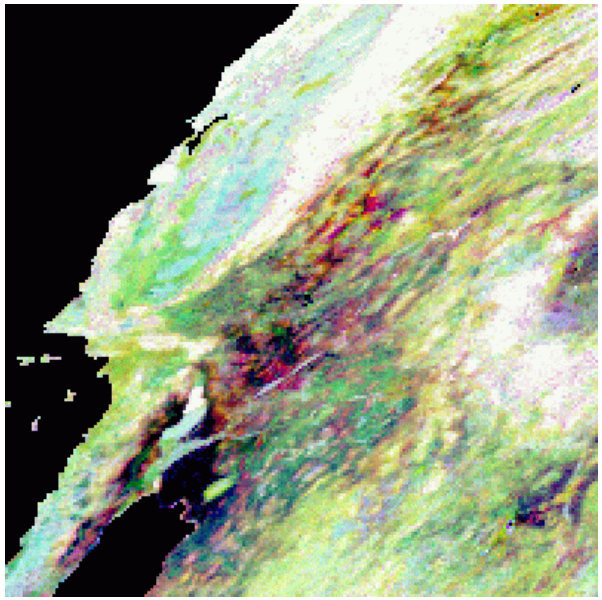

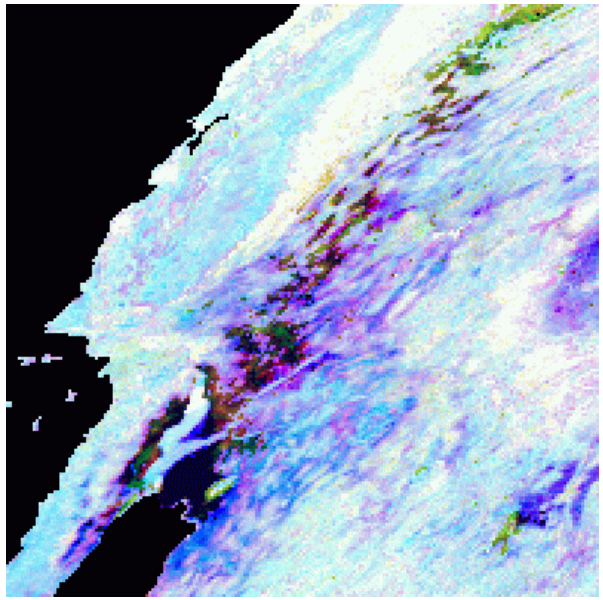

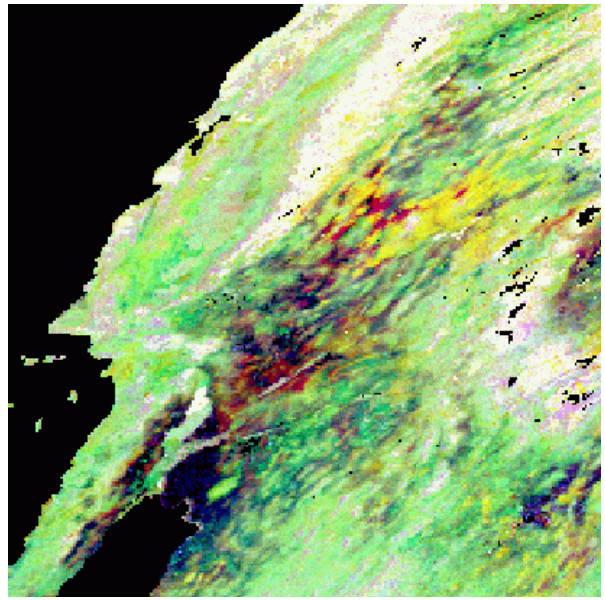

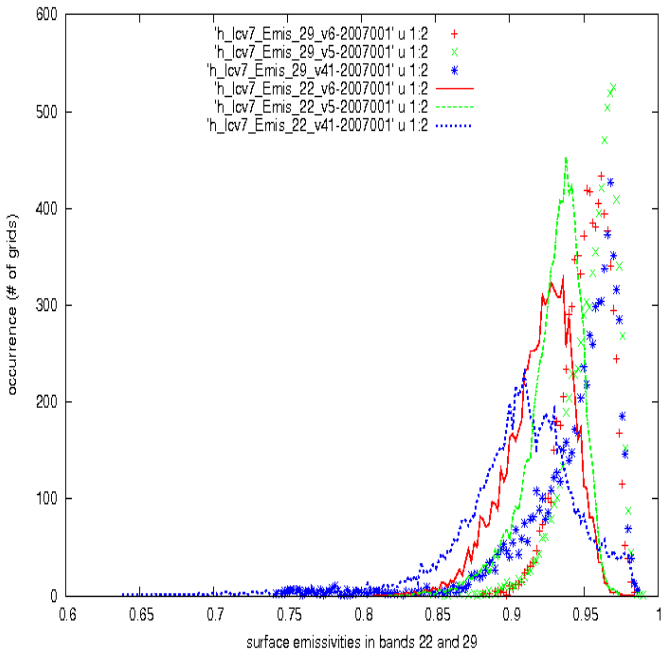

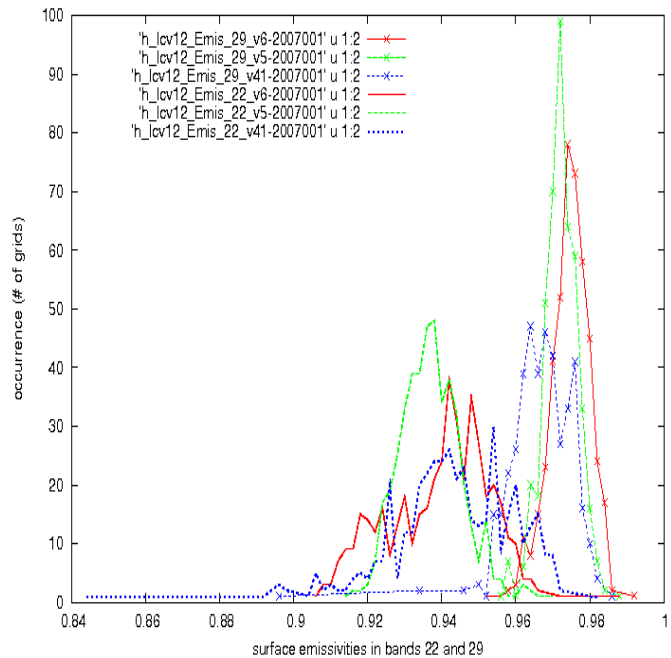

Over open shrub-lands (lcv7) in tile h08v05, the Emis_29 values in C5 are slightly higher than those in C6 but the Emis_22 values are relatively more higher in C5 than C6. The values of Emis_22 and Emis_29 in C41 extend to below 0.65 and 0.75, respectively. These seem too low. Overall, C6 emissivity composite is between those of C41 and C5. The spatial coverage of retrieved Emis values is full in the middle right portion in both C5 and C6. But in C41, there are many grids without valid emissivity values. Over croplands (lcv12) in tile h08v05, the Emis_22 & Emis_29 values in C6 are more closer to C5 than C41, the values in C41 are too low.

Comparison of the color composite with em22, em29 and 31 as RGB in tiles h22-26v05 in the C6 MYD11B1 (top) to C5 (middle) during 7/1-27/2003, and C41during 7/1-27/2007 (bottom)

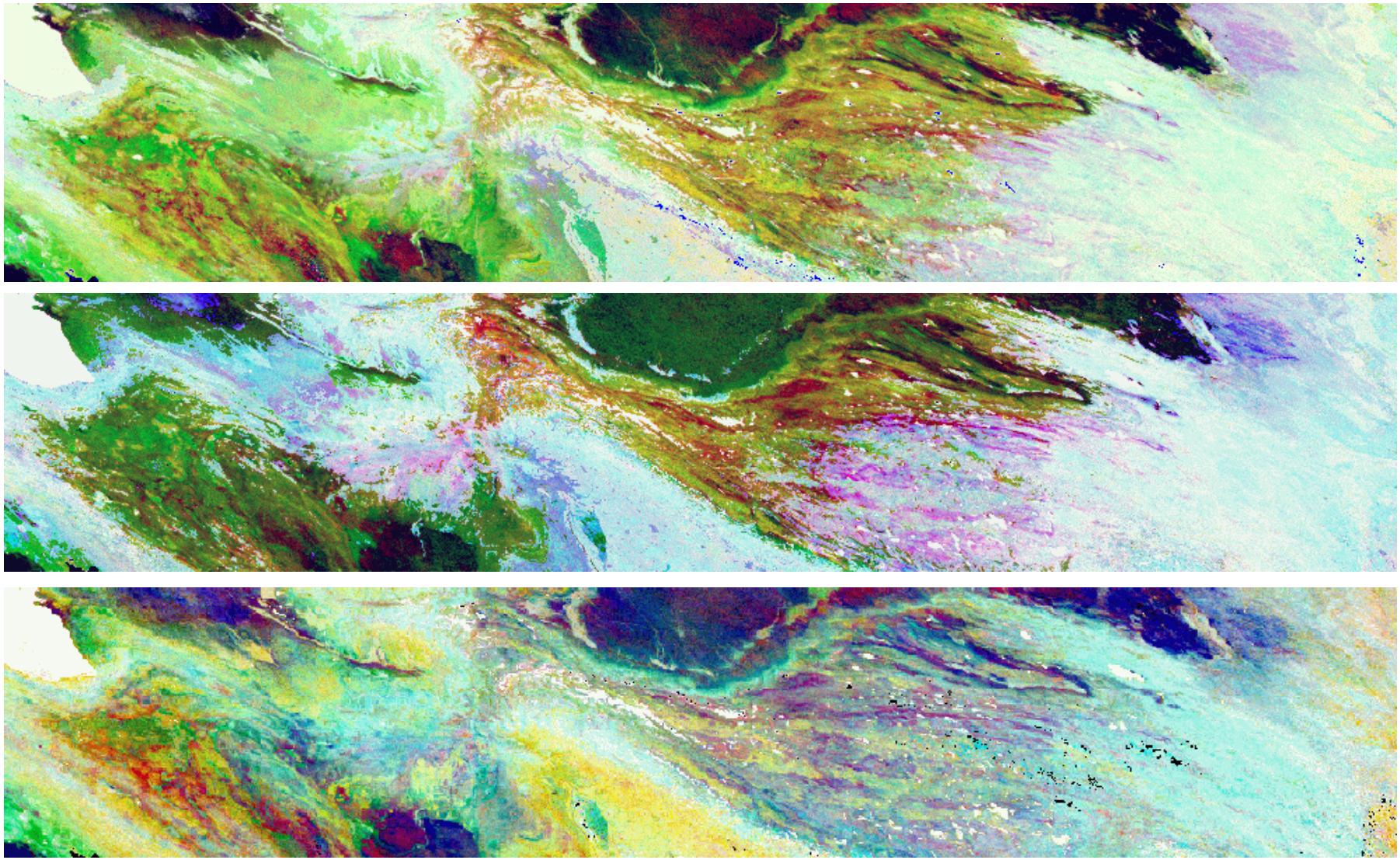

Over regions with higher emis values such as grass and croplands in the right portion, C6 is more closer to C5. In these regions (in this color), em31 values in C41 are relatively too low compared to em22 and em29 values. Over regions with low emis values such as in desert and arid areas, C6 is more closer to C41.

Is the seasonal change shown in the color composites with em22, em29 and 31 in the C6 MYD11B1 as RGB components between 1/1-24/2003 (left) and 7/1/27/2003 (right) real?

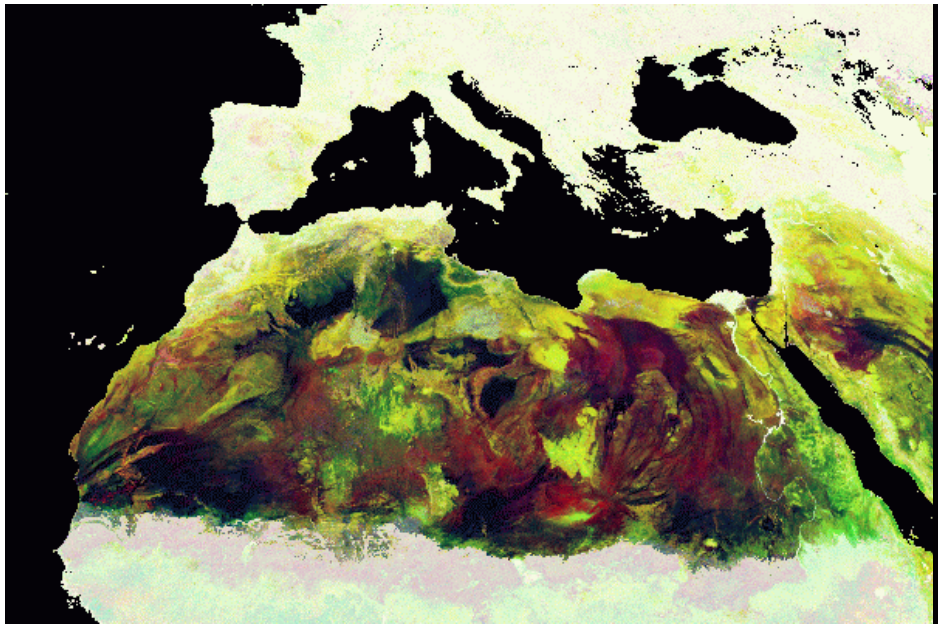

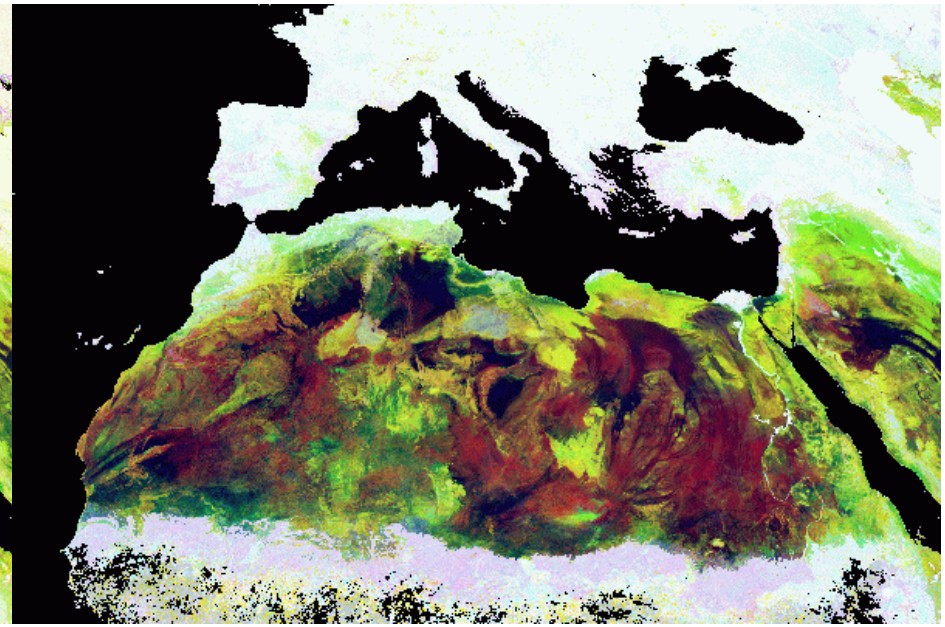

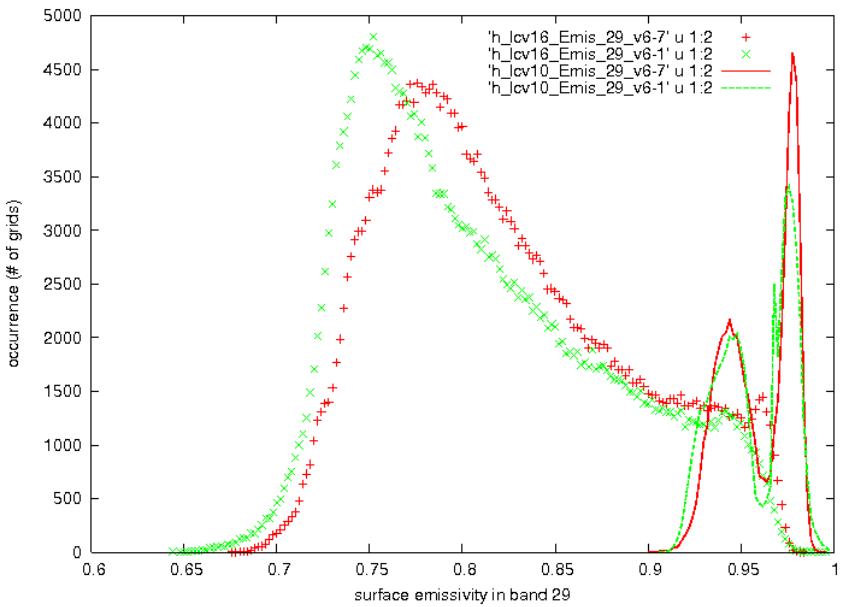

The histograms of Emis_29 values in grasslands (lcv10) and bare lands (lcv16) indicate that the values in July (red) are slightly higher than January (green). According to Kadomura H., (2005). 'Climate anomalies and extreme events in Africa in 2003, including heavy rains and floods that occurred during northern hemisphere summer', ***African Study Monographs***, Suppl.30: 165-181. The climatologic monthly averages of the total precipitation and rainy days over the 30-year period of 1976-2005 are higher in June-Sept. than in Jan.-Feb. in some places in Sahara such as Tamanrasset, see http://www.worldweather.org/122/c01362.htm.

Angular dependence in C6 band 29 emis values at selected grids in arid regions

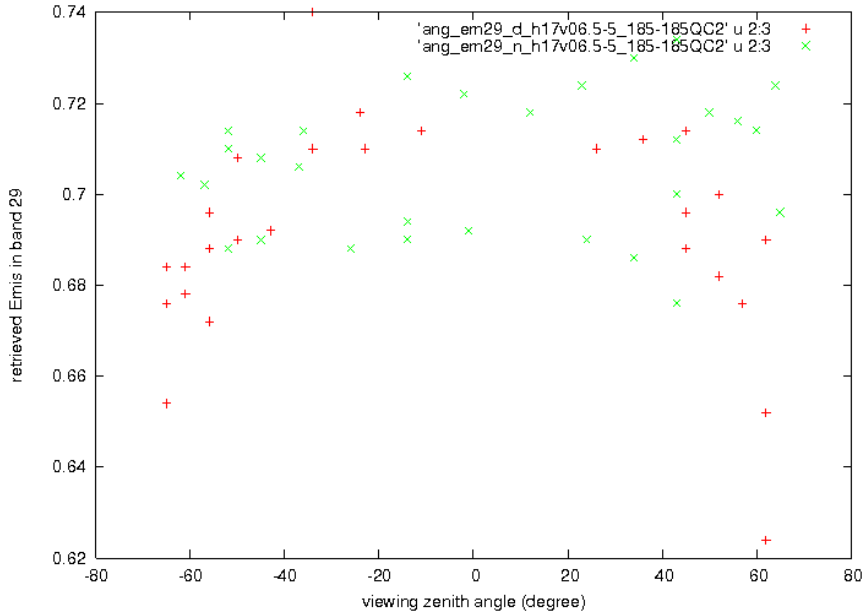

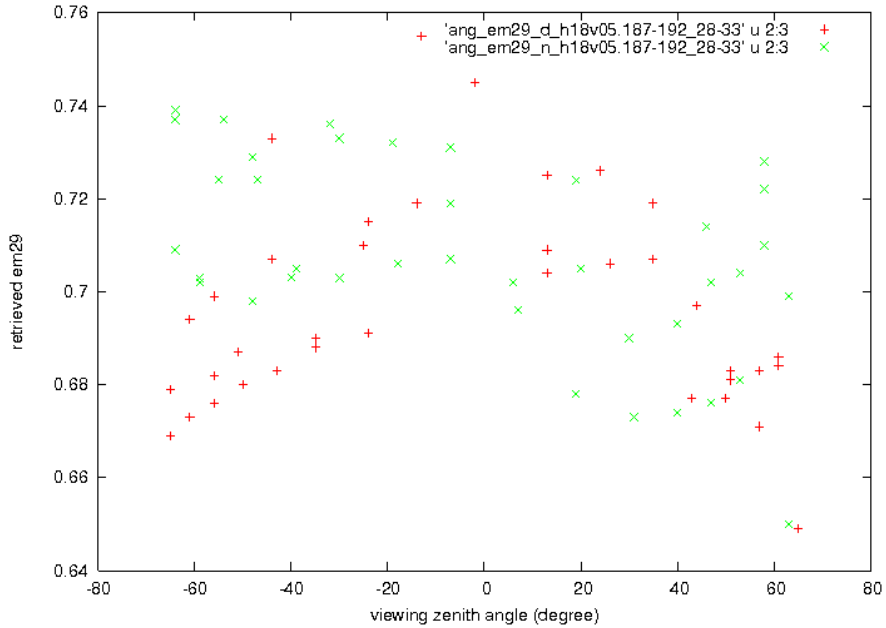

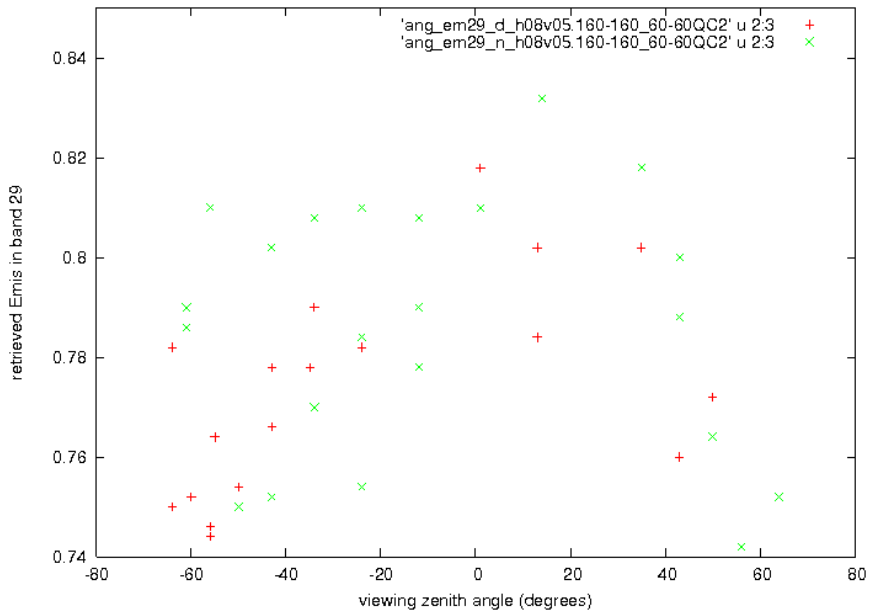

These plots indicate that the angular dependence in the retrieved band 29 emis values is, in general, consistent to the results in Fig. 9 of Tang, B. and Li, Z. -L.(2008) 'Retrieval of land surface bidirectional reflectivity in the mid-infrared from MODIS channels 22 and 23', *Inter. J. of Remote Sens.*, 29: 17, 4907-4925.

Note that it is not easy to trace the fluctuation in the data to the real change in surface moisture conditions or algorithm errors and/or cloud contamination.

Comparison of the color composite with em20, em22 and em29 as RGB components (top left), em31, em32 and 32 as RGB (top middle) in h16-21v04-07 in the C6 MYD11B1 product during 1/1-24/2003 to landcover (top right), NDVI (bottom left) and reflectance in b7/b4/b5 as RGB in MYD09 (bottom middle)

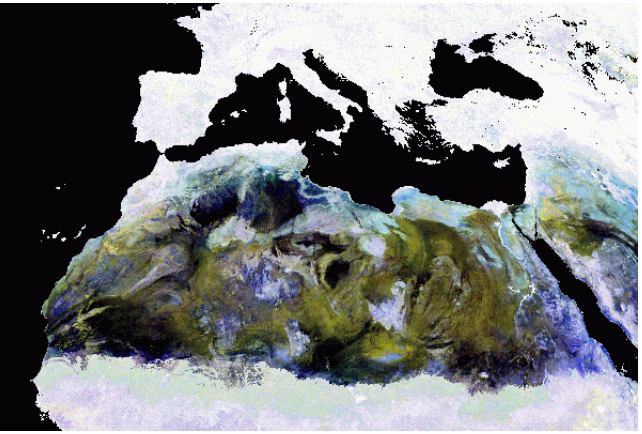
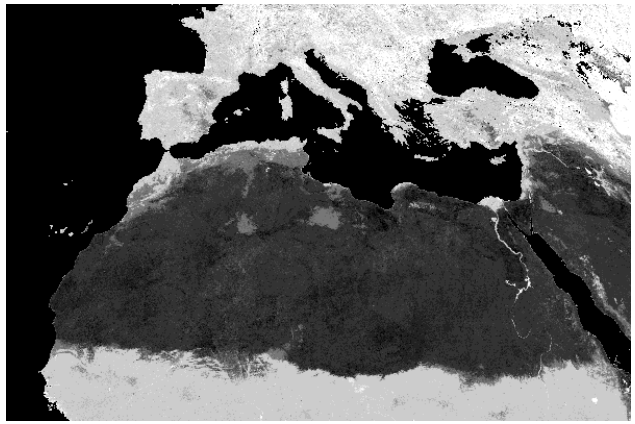
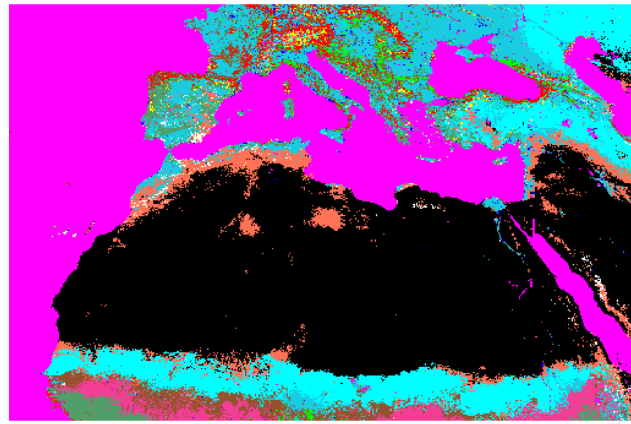
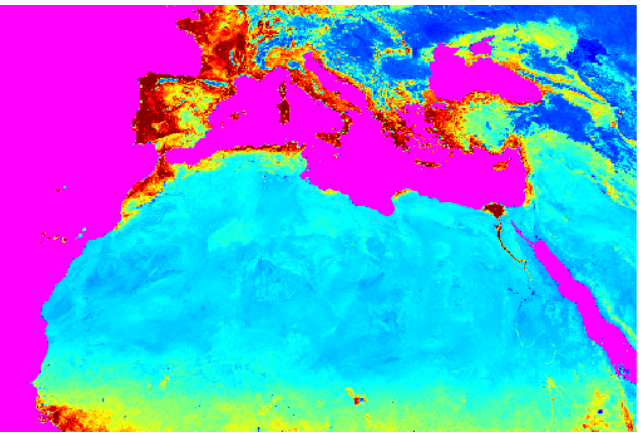
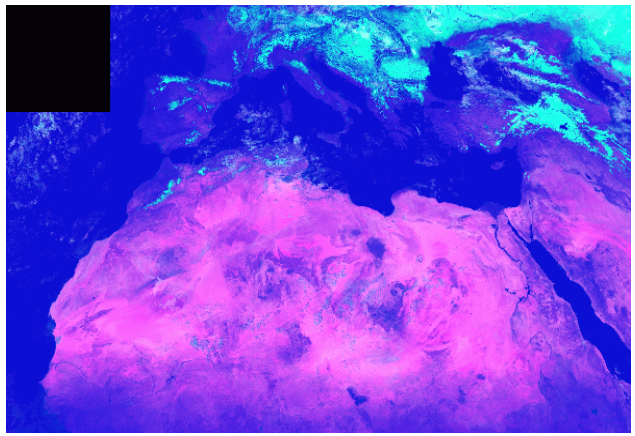

The correlation between emis values in bands 31/32 in M*D11B1 and the landcover is quite good. But the correlation between emis values in bands 20/22/29 in M*D11B1 and other MODIS land products are quite weak.

Work Plan

1. To deliver V6 codes for all the LST PGEs before late August 2012.

2. TIR BRDF retrieval in bands 20, 22 and 29 (in spectral range of 3.66-8.7μm) with multi-day Terra and Aqua MODIS data in arid regions will be compared to the angular dependence of the emissivities retrieved by the day/night algorithm and to the BRDF coefficients of band 7 (at 2.114μm) in the MODIS BRDF product.

3. Evaluate the model of split-window differential emissivity adjustment by comparing the brightness temperature difference in C6 MODIS bands 31 and 32 data to the simulation value estimated from atmospheric cwv and Ts-air to decide whether it is possible to improve the classification-based emissivity values for better LST retrieval in arid regions (for example at sites 40 and 42).

4. Science data analysis will be made for the correlations of LST/E data in the C6 with other independent data sets such as NDVI, ground measurement data of precipitation and soil moisture.

5. Radiance-based validation will be performed for the C6 Terra and Aqua MODIS LST products over different test sites world-wide.

6. To verify/confirm that the C6 MODIS LST/E product can replace C5 & C41.

A short list of references

Coll, C., Wan, Z., & Galve, J.M., (2009). Temperature-based and radiance-based validation for the V5 MODIS land-surface temperature product. *JGR,* 114, D20102, doi:10.1029/2009JD012038.

Wan, Z., (2008). New refinements and validation of the MODIS land-surface temperature/emissivity products. *Remote Sensing of Environment*, 112, 59-74.

Wan, Z., & Li, Z.-L., (2008). Radiance-based validation for the V5 MODIS land-surface temperature product. *International Journal of Remote Sensing*, 29, 5373-5395.

Coll, C., Caselles, V., Galve, J.M., Valor, E., Niclòs, R., Sánchez, J.M., & Rivas, R. (2005). Ground measurements for the validation of land surface temperatures derived from AATSR and MODIS data. *Remote Sensing of Environment*, 97, 288-300.

Tang, B.-H., Li, Z.-L., & Yuyun, B., (2009). Estimation of land surface directional emissivity in mid-infrared channel around 4.0μm from MODIS data, *Optics Express*, 17, 3173-3182.

Kadomura, H., (2005). Climate anomalies and extreme events in Africa in 2003, including heavy rains and floods that occurred during northern hemisphere summer, *African Study Monographs*, Suppl.30: 165-181.

Snyder, W.C., Wan, Z., Zhang, Y., & Feng, Y.-Z. (1998). Classification-based emissivity for land surface temperature measurement from space. *International Journal of Remote Sensing*, 19, 2753-2574.

Wan, Z., & Dozier, J. (1996). A generalized split-window algorithm for retrieving land-surface temperature from space. *IEEE Trans. Geoscience and Remote Sensing,* 34, 892–905.

Wan, Z., & Li, Z.-L. (1997). A physics-based algorithm for retrieving land-surface emissivity and temperature from EOS/MODIS data. *IEEE Trans. Geoscience and Remote Sensing*, 35, 980-996.

Wan, Z., Zhang, Y., Zhang, Y.Q., & Li, Z.-L. (2002). Validation of the land-surface temperature products retrieved from Moderate Resolution Imaging Spectroradiometer data. *Remote Sens. of Environ*, 83, 163-180.

Wan, Z., Zhang, Y., Zhang, Y.Q., & Li, Z.-L. (2004). Quality assessment and validation of the global land surface temperature. *International Journal of Remote Sensing*, 25, 261-274.

http://www.icess.ucsb.edu/modis/LstUsrGuide/usrguide.html